Rui Cheng,[1,2] Lexi Ding,[1,2] Xuemin He,[1,2] Yusuke Takahashi,[2,3] and Jian-xing Ma[1,2]

Interaction of PPARα With the Canonic Wnt Pathway in the Regulation of Renal Fibrosis

Diabetes 2016;65:3730–3743 | DOI: 10.2337/db16-0426

COMPLICATIONS

Peroxisome proliferator–activated receptor-α (PPARα) displays renoprotective effects with an unclear mechanism. Aberrant activation of the canonical Wnt pathway plays a key role in renal fibrosis. Renal levels of PPARα were downregulated in both type 1 and type 2 diabetes models. The PPARα agonist fenofibrate and overexpression of PPARα both attenuated the expression of fibrotic factors, and suppressed high glucose–induced or Wnt3a-induced Wnt signaling in renal cells. Fenofibrate inhibited Wnt signaling in the kidney of diabetic rats. A more renal prominent activation of Wnt signaling was detected both in PPARα$^{-/-}$ mice with diabetes or obstructive nephropathy and in PPARα$^{-/-}$ tubular cells treated with Wnt3a. PPARα did not block the transcriptional activity of β-catenin induced by a constitutively active mutant of lipoprotein receptor–related protein 6 (LRP6) or β-catenin. LRP6 stability was decreased by overexpression of PPARα and increased in PPARα$^{-/-}$ tubular cells, suggesting that PPARα interacts with Wnt signaling at the Wnt coreceptor level. 4-Hydroxynonenal–induced reactive oxygen species production, which resulted in LRP6 stability, was suppressed by overexpression of PPARα and dramatically enhanced in PPARα$^{-/-}$ tubular cells. Diabetic PPARα$^{-/-}$ mice showed more prominent NADPH oxidase-4 overexpression compared with diabetic wild-type mice, suggesting that the inhibitory effect of PPARα on Wnt signaling may be ascribed to its antioxidant activity. These observations identified a novel interaction between PPARα and the Wnt pathway, which is responsible, at least partially, for the therapeutic effects of fenofibrate on diabetic nephropathy.

Diabetic nephropathy (DN) occurs in 30–40% of patients with diabetes (1,2). Without therapeutic intervention, overt nephropathy will develop in 80% of individuals with type 1 diabetes with sustained microalbuminuria in 10–15 years (2). DN accounts for 40% of newly diagnosed end-stage renal disease in the U.S. (3). A better understanding of the pathogenesis of DN could facilitate the development of novel and effective therapeutic strategies.

Peroxisome proliferator–activated receptor-α (PPARα) is a ligand-dependent nuclear receptor, regulating lipid metabolism (4). PPARα can be activated by exogenous compounds, such as fibrates, and also by endogenous ligands, including fatty acids and prostaglandins (4). PPARα is mainly expressed in tissues with high mitochondrial and β-oxidation activities, including the liver, renal cortex, intestinal mucosa, and heart. The known functions of PPARα are primarily the regulation of fatty acid oxidation. Two independent, prospective clinical studies, the Fenofibrate Intervention and Event Lowering in Diabetes (FIELD) study and the Action to Control Cardiovascular Risk in Diabetes (ACCORD) study, reported that fenofibrate, a PPARα agonist, has robust therapeutic effects on DN in human patients with type 2 diabetes, suggesting that PPARα is a potential target for the treatment of DN (5–7). Activation of PPARα was found to ameliorate DN in diabetic animal models due to its antifibrosis and anti-inflammatory effects (8). PPARα deficiency has been shown to aggravate DN by increasing extracellular matrix formation and inflammation in the kidney (9). However, the molecular mechanism underlying its antifibrogenic and anti-inflammatory effects remains elusive.

[1]Department of Physiology, University of Oklahoma Health Sciences Center, Oklahoma City, OK
[2]Harold Hamm Diabetes Center, University of Oklahoma Health Sciences Center, Oklahoma City, OK
[3]Department of Medicine, University of Oklahoma Health Sciences Center, Oklahoma City, OK
Corresponding author: Jian-xing Ma, jian-xing-ma@ouhsc.edu.

Received 1 April 2016 and accepted 4 September 2016.
This article contains Supplementary Data online at http://diabetes.diabetesjournals.org/lookup/suppl/doi:10.2337/db16-0426/-/DC1.

The canonical Wnt pathway regulates multiple physiological and pathological processes including angiogenesis, inflammation, and fibrosis. The activation of Wnt signaling is triggered by the binding of Wnt ligands to a coreceptor complex consisting of a frizzled (Fz) receptor and low-density lipoprotein receptor–related protein (LRP) 5/6, leading to activation of β-catenin, a transcription factor, which subsequently activates the transcription of Wnt target genes, including multiple factors associated with angiogenesis, fibrosis, and inflammation (10). Other groups and we have independently shown (11–13) that the Wnt pathway is aberrantly activated in the kidneys of patients with diabetes and in diabetic animal models. We have demonstrated that Wnt ligands and receptors are significantly upregulated in diabetic kidneys and that hyperglycemia-induced oxidative stress contributes to the overactivation of Wnt signaling in diabetic complications (12). Inhibition of the Wnt pathway using a monoclonal antibody blocking LRP6 ameliorated proteinuria and renal fibrosis in a type 1 diabetes model, suggesting that Wnt signaling plays a role in DN-associated renal inflammation and fibrosis (12).

Several studies demonstrated the cross talk between PPARγ and the Wnt signaling pathway in adipogenesis, osteoblastogenesis, kidney diseases, and cancer. However, the regulatory effect of PPARα on the canonical Wnt signaling pathway has not been well defined. In this study, we explored a novel interaction between PPARα and the Wnt pathway, which is responsible, at least in part, for the anti-inflammatory and antifibrogenic effects of PPARα and its agonists in DN.

RESEARCH DESIGN AND METHODS

Streptozotocin-Induced Diabetic Animal Model

Diabetes was induced as described in a previous report (14). Briefly, 8-week-old Brown Norway rats (Charles River Laboratories, Wilmington, MA) were fasted overnight and then received a single intraperitoneal injection of streptozotocin (STZ) (Sigma-Aldrich, St. Louis, MO) at a dose of 55 mg/kg. Eight-week-old PPARα$^{-/-}$ mice with a C57BL/6J background and wild-type (Wt) C57BL/6J mice (The Jackson Laboratory, Bar Harbor, ME) received five consecutive daily intraperitoneal injections of STZ at a dose of 55 mg/kg. Blood glucose levels were measured 72 h after STZ injection for the rat or 1 week after for the mouse after the last STZ injection. Animals with blood glucose levels >350 mg/dL were defined as diabetic animals. All of the experiments were approved by the Institutional Animal Care and Use Committee of The University of Oklahoma.

At 6 weeks of diabetes, diabetic rats were randomly assigned into two groups and fed regular chow or special chow containing 0.1% fenofibrate (LabDiet; TestDiet, Fort Worth, TX) for another 6 weeks. Age-matched nondiabetic animals were used as normal controls.

Unilateral Ureter Obstruction Model

PPARα$^{-/-}$ mice were crossed with the BAT-*gal* Wnt reporter mice (The Jackson Laboratory) to generate PPARα$^{-/-}$ or Wt mice that carried the BAT-*gal* transgene. Mice received the unilateral ureter obstruction (UUO) operation in the left kidney at the age of 8 weeks, as described previously (15). Mice were euthanized on the 7th day after the operation, and the kidney was dissected and sectioned for X-gal staining.

Measurement of Urine Albumin and Creatinine

Metabolic cages were used for collection of 24-h urine samples. Levels of urine albumin and creatinine were measured and calculated as described previously (12).

X-Gal Staining

X-Gal staining was performed in kidney sections as previously described (16). Briefly, mice were perfused with 4% paraformaldehyde in PBS containing 2 mmol/L $MgCl_2$ (pH 7.4). The postobstructive kidney was dissected and postfixed in 4% paraformaldehyde for an additional 2 h, followed by dehydration in 30% sucrose overnight. Tissues were embedded in OCT, and cryosections of 5–30 μm were cut. Sections were washed in PBS with 0.01% sodium deoxycholate and 0.02% NP-40 for 2 h, and stained in X-gal solution (1 mg/mL X-gal, 5 mmol/L potassium ferricyanide, and 5 mmol/L potassium ferrocyanide in PBS; Sigma-Aldrich) for 6 h at 37°C. Images were visualized and captured using an Olympus microscope.

Immunohistochemistry

Five-micrometer sections were prepared from a paraffin-embedded kidney for immunohistochemistry as described previously (12). Briefly, kidney sections were blocked with normal goat serum and the Avidin/Biotin Blocking Kit (Vector Laboratories, Burlingame, CA) according to the manufacturer protocol. To quantify the expression levels of renal collagen IV, fibronectin, and LRP6, sections were incubated separately with anti–collagen IV (Millipore, Billerica, MA), anti-fibronectin (Santa Cruz Biotechnology, Dallas, TX), anti–β-catenin (Santa Cruz Biotechnology), anti-PPARα (Abcam, Eugene, OR), and anti-LRP6 (in-house antibody) (17) antibodies. ABC reagent (Vector Laboratories) was used, and the color was developed by DAB substrate (BD Biosciences, San Jose, CA) according to manufacturer instructions.

Cell Culture and Treatment

Human renal proximal tubule cells (HRPTCs) were purchased from the American Type Culture Collection (ATCC; Manassas, VA) and cultured according to the recommendations of ATCC. HKC-8 cells, a cell line derived from human renal proximal tubular epithelial cells, were from Dr. L. Racusen (The Johns Hopkins University, Baltimore, MD) and were cultured in DMEM/F12 medium with 5% FBS (Life Technologies, Grand Island, NY), as described previously (18). L-cells and L-cells expressing Wnt3a were obtained from the ATCC and maintained in DMEM supplemented with 10% FBS cultured following recommendations from ATCC. Wnt3a conditioned medium (WCM) and the control medium from L-cells were collected according to the manufacturer protocol. Tubular cells were starved in 0.2% FBS (HRPTCs) or serum-free medium (HKC-8 cells)

overnight before treatment. Cells were treated with high-glucose medium containing 30 mmol/L D-glucose (Sigma-Aldrich) or control low-glucose medium containing 25 mmol/L L-glucose plus 5 mmol/L D-glucose (Sigma-Aldrich) for the indicated time. Recombinant human transforming growth factor-β1 (TGF-β1) was from R&D Systems (Minneapolis, MN). Adenovirus expressing PPARα (Ad-PPARα) was generated as described previously (19). Cells were infected with Ad-PPARα or control Ad, as described previously (12,20).

Culture of Primary Mouse Renal Proximal Tubular Cells

Mouse primary proximal tubular cells were cultured from 21-day-old PPARα$^{-/-}$ mice or their genetic background–matched Wt littermates according to a documented protocol (21). The cells from these mice were isolated side by side and used at the same passage. Proximal tubular fragments were maintained in a renal proximal tubular cells special medium (ATCC) supplement with 5% FBS, 10 ng/mL EGF (R&D Systems), 1% antibiotic-antimycotic, and insulin-transferrin-selenium (Life Technologies), and seeded in collagen-coated dishes in a 37°C humidified incubator with 5% CO_2. Culture medium was changed 48 h after seeding, and then changed every 2 days. Cells at passages 1–4 were used in this study. Mouse primary proximal tubular cells were identified at passage 1 by immunostaining with the antibody against sodium-dependent glucose cotransporter 1 (Millipore). Commercial HRPTCs were used as the positive control for the immunostaining.

Luciferase Assay

The transcriptional activity of β-catenin was measured by luciferase assay, as described previously (22).

Measurement of the Reactive Oxygen Species

Cells in 24-well plates were treated with different concentrations of 4-hydroxynonenal (4-HNE) for 2 h. Intracellular reactive oxygen species (ROS) was quantified by CM-H_2DCF-DA staining (Molecular Probes/Invitrogen, Carlsbad, CA) according to manufacturer instructions.

Extraction of Nuclear Protein

Nuclear fractions from renal cortical tissues were extracted using the Fraction PREP Cell Fractionation Kit (BioVision, Mountain View, CA) following manufacturer instructions.

Western Blot Analysis

Cells were lysed using 1× SDS lysis buffer (62.5 mmol/L Tris-HCl [pH 6.8], 2% SDS, 10% glycerol, 0.1% bromophenol blue, 1× protein inhibitor cocktails [ThermoFisher Scientific, Rockford, IL], 10 mmol/L NaF [Sigma-Aldrich], and 2 mmol/L sodium orthovanadate [Sigma-Aldrich]). Renal cortical lysates were prepared by adding 100 μL of tissue lysis buffer (50 mmol/L Tris-HCl, pH 7.8, 5 mmol/L EDTA, 0.1% SDS, 1% NP-40, 2.5% glycerol, 100 mmol/L NaCl, and 1 mmol/L fresh phenylmethylsulfonyl fluoride, and 1× protein inhibitor cocktails, 10 mmol/L NaF and 2 mmol/L sodium orthovanadate) per 10 mg of tissue. After sonication, the supernatant of the tissue homogenate was separated by centrifugation at 14,000 × *g* at 4°C for 15 min. Protein concentration was determined using BCA assay (Thermo Fisher). Fifty micrograms of protein was subjected to Western blot analysis, as published previously (23). The following primary antibodies were used: anti–phosphorylated LRP6 (p-LRP6) (Ser1490, 1:1,000; Cell Signaling Technology, Danvers, MA), anti-LRP6 (1:2,000; in-house generated), anti–nonphosphorylated (N-p)-β-catenin (1:1,000, Cell Signaling Technology), anti–β-catenin (1:3,000; Santa Cruz Biotechnology), anti–connective tissue growth factor (CTGF; 1:500; Santa Cruz Biotechnology), antifibronectin (1:100; Santa Cruz Biotechnology), anti-PPARα (1:500; Santa Cruz Biotechnology), anti–NADPH oxidase-4 (NOX4) (1:3,000; Abcam, Cambridge, MA), anti–β-actin (1:50,000; Sigma-Aldrich).

Statistical Analysis

Data are expressed as the mean ± SD. Statistical analysis was performed using Student *t* test for the comparison between two groups, or using ANOVA for the analysis among more than two groups. A *P* value of <0.05 was considered to be statistically significant.

RESULTS

Activation of PPARα Ameliorates Renal Fibrosis in Diabetic Kidney

PPARα expression was evaluated in the kidneys of STZ-induced diabetic rats (type 1 diabetes) at 12 weeks after diabetes onset, and *db/db* mice (type 2 diabetes) at 6 months of age. The expression of PPARα was significantly decreased in the renal cortex of diabetic animals at both the protein and mRNA levels (Fig. 1*A*–*F*).

To evaluate the protective effect of PPARα on renal fibrosis, STZ-induced diabetic rats at 6 weeks after diabetic onset were fed with special chow containing 0.1% fenofibrate for another 6 weeks. Fenofibrate treatment significantly reduced albuminuria in diabetic rats without changing body weight and blood glucose concentration, compared with diabetic rats with regular chow (Fig. 1*G* and Supplementary Fig. 1*A* and *B*). Fenofibrate significantly decreased collagen IV and fibronectin accumulation in kidneys of diabetic rats (Fig. 1*H*). The overexpression of TGF-β1, fibronectin, and CTGF was attenuated by fenofibrate in the diabetic kidneys (Fig. 1*I* and *J*). These results suggested that activation of PPARα has an antifibrotic activity in DN models.

Activation of PPARα Attenuates Renal Fibrosis Through Blocking the Canonic Wnt Signaling Pathway

The proximal tubule is an important player in renal hypertrophy, inflammation, and fibrosis in DN by generating and secreting fibrosis-related proteins, such as fibronectin, CTGF, TGF-β, and collagen IV (24). The expression of CTGF and fibronectin in primary HRPTCs was upregulated by high glucose, compared with those in the control cells treated with low glucose. Fenofibrate significantly suppressed high glucose–induced CTGF and fibronectin expression in a concentration-dependent manner (Fig. 2*A*–*C*). Overexpression of PPARα by an Ad-PPARα significantly attenuated high glucose–induced expression of CTGF and

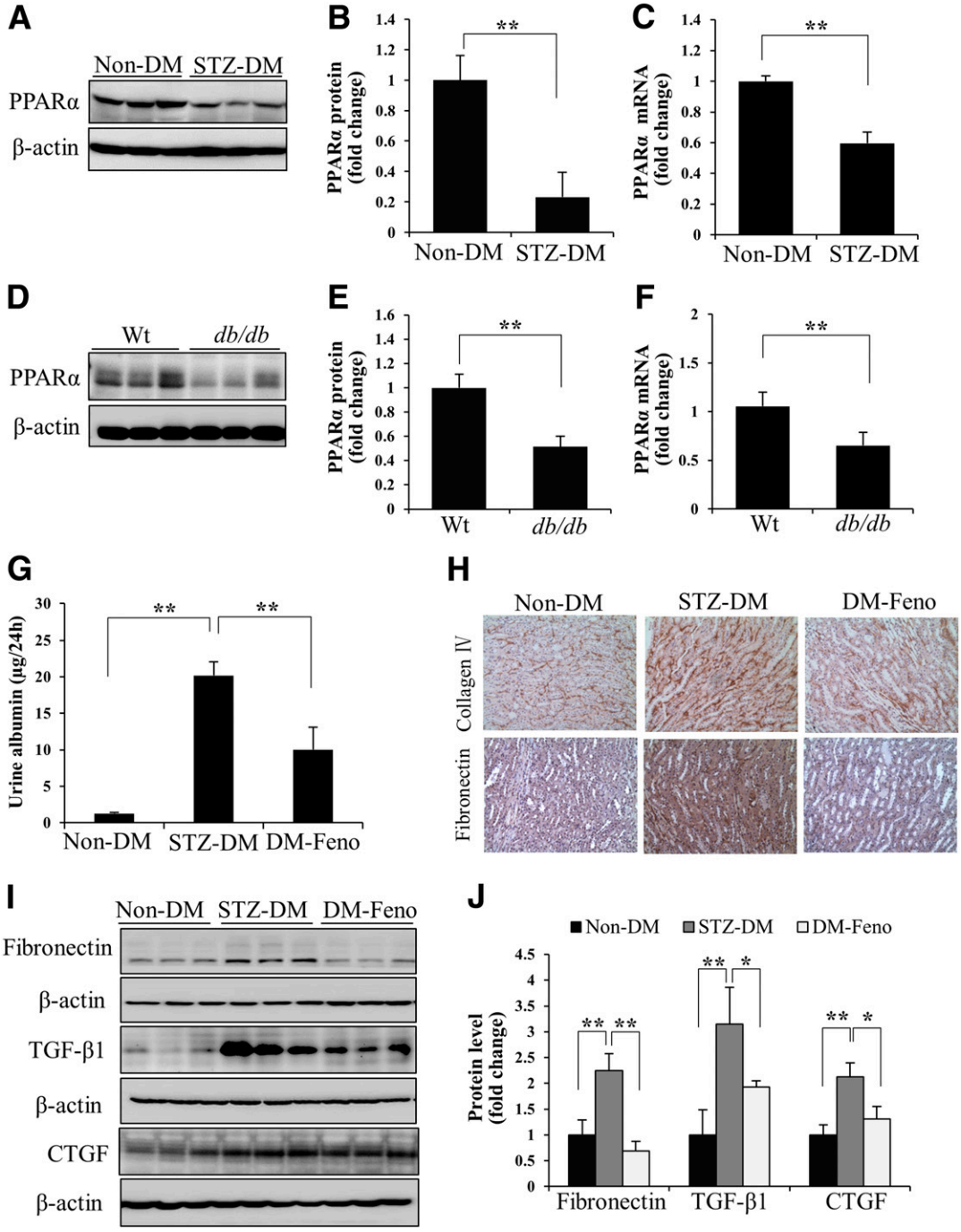

Figure 1—Activation of PPARα ameliorates renal fibrosis in diabetic kidney. Representative Western blots (*A*), semiquantitative densitometry analyses (*B*), and real-time RT-PCR results (*C*) show PPARα protein and mRNA levels in the renal cortex of nondiabetic rats (Non-DM) and STZ-induced diabetic rats (STZ-DM) at 12 weeks after the onset of diabetes. n = 4–7. Representative Western blots (*D*), semiquantitative analyses (*E*), and real-time RT-PCR results (*F*) show PPARα protein and mRNA levels in the renal cortex of *db/db* mice and age-matched Wt mice at the age of 6 months. n = 5. *G*: Albumin levels in 24-h urine samples from Non-DM–induced and STZ-induced diabetic rats with fenofibrate chow (DM-Feno) or control chow (STZ-DM) were measured by ELISA. *H*: Representative images of immunohistochemistry show the expression of collagen IV and fibronectin in Non-DM, STZ-DM, and DM-Feno (original magnification ×200). Levels of fibronectin, CTGF, and TGF-β1 in renal cortex lysates were determined by Western blot analysis (*I*) and semiquantitative analysis (*J*) in Non-DM, STZ-DM, and DM-Feno rats. Values are reported as the mean ± SD: n = 4 in Non-DM and STZ-DM; n = 6 in DM-Feno. $^*P < 0.05$ and $^{**}P < 0.01$.

fibronectin (Fig. 2*D–F*). These results demonstrate an antifibrogenic activity of PPARα in renal cells under diabetes conditions.

We have previously reported a pathogenic role for the overactivation of canonic Wnt signaling in renal inflammation and fibrosis in DN (12). WCM-induced fibronectin

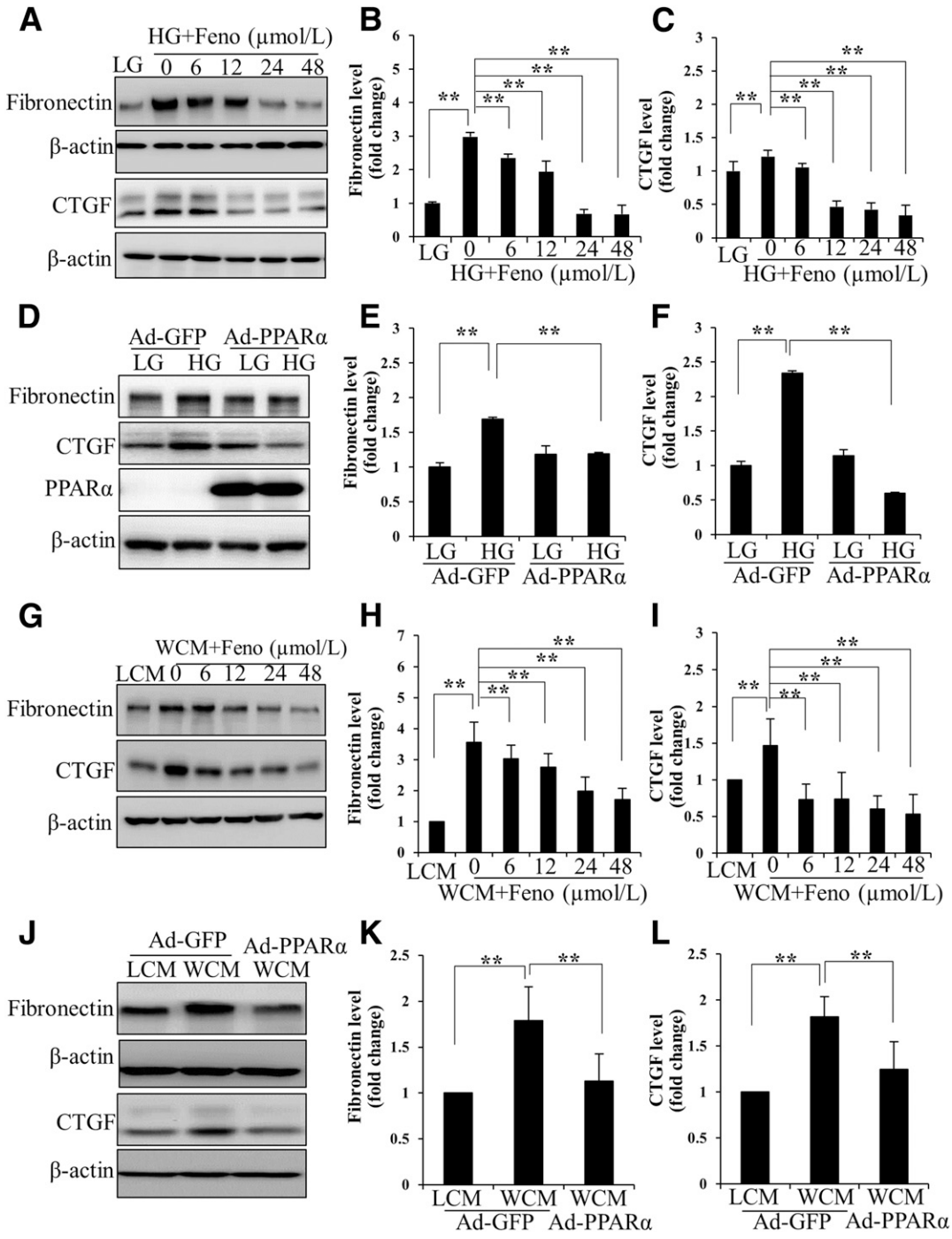

Figure 2—PPARα attenuates renal fibrosis in proximal tubular cells. Representative Western blots (*A*) and densitometry analyses of fibronectin (*B*) and CTGF (*C*) in primary HRPTCs treated with high glucose (HG; 30 mmol/L D-glucose) and indicated concentrations of fenofibrate (Feno) for 72 h. Low glucose (LG; 25 mmol/L L-glucose plus 5 mmol/L D-glucose) was used as a negative control. Primary HRPTCs were infected with Ad-PPARα for 24 h, with Ad-expressing green fluorescent protein (Ad-GFP) as a control, and then treated with HG for another 72 h. Levels of fibronectin and CTGF were determined by Western blot analysis (*D*) and semiquantified by densitometry (*E* and *F*). Levels of fibronectin and CTGF were measured with Western blot analyses (*G*) and quantified (*H* and *I*) in primary HRPTCs treated with WCM, and indicated concentrations of fenofibrate for 24-h L-cell medium (LCM) were used as a negative control. Primary HRPTCs were infected with Ad-PPARα and then treated with WCM for 24 h. Representative Western blots (*J*) and densitometry analyses (*K* and *L*) show the expression of fibronectin and CTGF in HRPTCs. Values are reported as the mean ± SD, $n = 3$. $^{**}P < 0.01$.

and CTGF expression was significantly inhibited by fenofibrate and Ad-PPARα (Fig. 2*G–L*). Fenofibrate or Ad-PPARα significantly attenuated high glucose– or WCM-induced upregulation of p-LRP6, a major coreceptor in Wnt signaling, and N-p-β-catenin, an effector of canonical Wnt signaling, in renal tubular cells (Fig. 3). Consistently, a

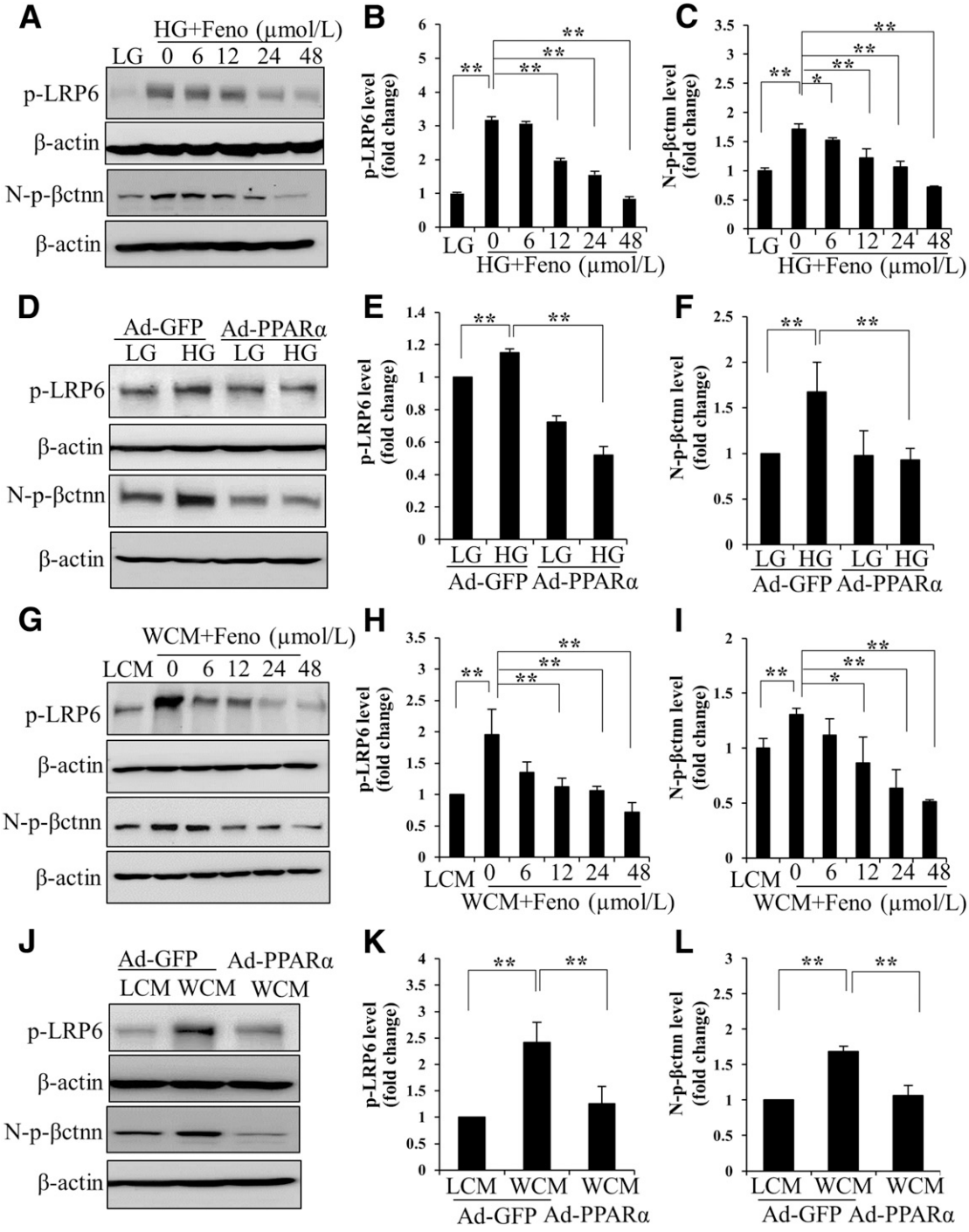

Figure 3— Inhibitory effects of PPARα on high glucose–induced and Wnt3a-induced activation of Wnt signaling. Representative Western blots (*A*) and densitometry analyses of p-LRP6 (*B*) and N-p-β-catenin (N-p-βctnn) (*C*) in HRPTCs exposed to 30 mmol/L D-glucose (high glucose [HG]), with 5 mmol/L D-glucose + 25 mmol/L L-glucose (low glucose [LG]) as a control, and treated with indicated concentrations of fenofibrate (Feno) for 24 h. Levels of p-LRP6 and N-p-βctnn were determined in HRPTCs treated with HG and Ad-PPARα for 24 h by Western blot (*D*) and densitometry analyses (*E* and *F*). Levels of p-LRP6 and N-p-βctnn were measured by Western blot analysis (*G*) and densitometry analysis (*H* and *I*) in HRPTCs treated with WCM, and indicated concentrations of fenofibrate for 12 h in L-cell medium (LCM) was used as a negative control. Representative Western blots (*J*) and densitometry analyses (*K* and *L*) show changed levels of p-LRP6 and N-p-βctnn in HRPTCs infected with Ad-PPARα treated with WCM for 12 h. Ad-GFP, Ad-expressing green fluorescent protein. Values are reported as the mean ± SD, $n = 3$. $^{*}P < 0.05$; $^{**}P < 0.01$.

luciferase-based promoter assay demonstrated that both fenofibrate and Ad-PPARα dramatically inhibited the WCM-induced transcriptional activity of β-catenin (Fig. 4). The inhibitory effect of PPARα on the canonic Wnt pathway was further confirmed in the kidneys of diabetic rats. As shown by elevated levels of LRP6 and nuclear levels of

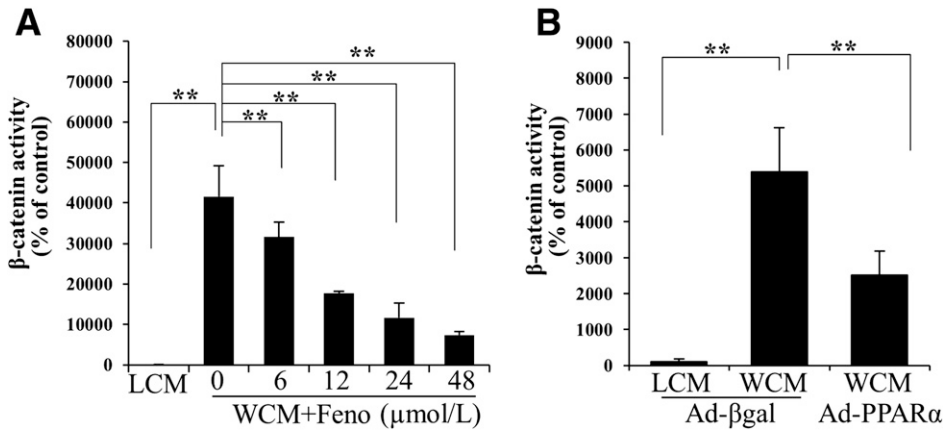

Figure 4—Inhibitory effects of PPARα on Wnt3a-induced transcriptional activity of β-catenin. Luciferase assay was used to quantify the effects of fenofibrate (Feno) (*A*) and overexpression of Ad-PPARα (*B*) on WCM-induced transcriptional activity of β-catenin in tubular cells. L-cell conditioned medium (LCM) and Ad-expressing β-galactosidase (Ad-βgal) were used as controls. Values are reported as the mean ± SD, $n = 4$. $^{**}P < 0.01$.

β-catenin, the canonic Wnt pathway was significantly activated in the kidney of STZ-induced diabetic rats. Fenofibrate chow attenuated the activation of the Wnt pathway in the STZ-induced diabetic rat kidneys (Fig. 5*A* and *B*). The effect of fenofibrate on LRP6 levels was also studied by immunostaining kidney sections (Fig. 5*C*). These results suggested that PPARα negatively regulated the canonic Wnt pathway.

PPARα Deficiency Results in More Prominent Activation of the Canonic Wnt Pathway and More Severe DN in Diabetic Animals

To evaluate the inhibitory effects of PPARα on Wnt signaling activation in vivo, diabetes was induced by STZ in PPARα$^{-/-}$ mice and age-matched and genetic background–matched Wt mice. PPARα$^{-/-}$ mice with 24 weeks of STZ-induced diabetes showed more severe proteinuria and dramatically enhanced renal expression of fibronectin, compared with the diabetic Wt mice (Fig. 5*D* and *E*), which is consistent with the findings of a previous report (9). However, there was no difference in body weights and blood glucose concentrations between diabetic PPARα$^{-/-}$ mice and Wt mice (Supplementary Fig. 1*C* and *D*). Interestingly, diabetic PPARα$^{-/-}$ mice showed more prominent increases of p-LRP6 and N-p-β-catenin levels in the kidney, suggesting higher Wnt signaling activities, compared with diabetic Wt mice (Fig. 5*E* and *F*). There were no significant differences in these Wnt signaling components or proteinuria between nondiabetic Wt mice and PPARα$^{-/-}$ mice. These results indicated that PPARα deficiency contributes to the activation of the canonic Wnt pathway induced by diabetic conditions.

The relationship between PPARα and the canonic Wnt pathway was further studied using the transgenic BAT-*gal* mouse, a Wnt signaling reporter mouse line that expresses the β-galactosidase reporter gene under the control of a promoter containing β-catenin/T-cell factor/lymphoid enhancer factor binding sites (25). PPARα$^{-/-}$ mice were crossed with BAT-*gal* mice to generate PPARα$^{-/-}$ mice carrying the BAT-*gal* transgene. To activate Wnt signaling in the kidney, these mice were subjected to the UUO, a commonly used model for renal fibrosis study. It was previously reported (26,27) that the canonic Wnt pathway was significantly activated in the UUO kidneys. X-Gal staining performed at 7 days after UUO operation showed significantly higher β-catenin transcriptional activities in the obstructive kidney of PPARα$^{-/-}$/BAT-*gal* mice, compared with those of their Wt/BAT-*gal* littermates with UUO (Fig. 5*G*). These results indicated that the activation of PPARα has an inhibitory effect on the canonic Wnt pathway in the kidney.

Primary murine proximal tubular cells were isolated and verified with immunostaining using an antibody against sodium–glucose cotransporter 1, a specific proximal tubular cell marker (Supplementary Fig. 2). PPARα$^{-/-}$ tubular cells demonstrated more prominent upregulation of p-LRP6, N-p-β-catenin, and fibronectin levels induced by high glucose, compared with Wt cells (Fig. 6*A* and *B*). WCM also induced more prominent increases of p-LRP6 levels and transcriptional activity of β-catenin in PPARα$^{-/-}$ cells compared with Wt cells (Fig. 6*C*–*E*). There were no differences in fibronectin expression and p-LRP6 levels between PPARα$^{-/-}$ cells and Wt cells with L-glucose or control L-cell medium treatment.

PPARα Does Not Inhibit the Transcriptional Activity of β-Catenin Induced by a Constitutively Active Mutant of LRP6 or β-Catenin

To delineate the mechanism by which PPARα suppresses the canonic Wnt pathway, a constitutively active LRP6 mutant lacking the extracellular domain (LRP6ΔN) (28,29) and a constitutively active β-catenin mutant with Serine37 substituted by Alanine (S37A) (12) were used. Both LRP6ΔN and S37A induced significant increases of the transcriptional activity of β-catenin in the absence of Wnt ligands (Fig. 7*A* and *B*). Although Ad-PPARα blocked the β-catenin transcriptional activity induced by Wnt ligand, Ad-PPARα had no inhibitory effect on LRP6ΔN- or S37A-induced transcriptional activity of β-catenin (Fig. 7*A* and *B*). These results

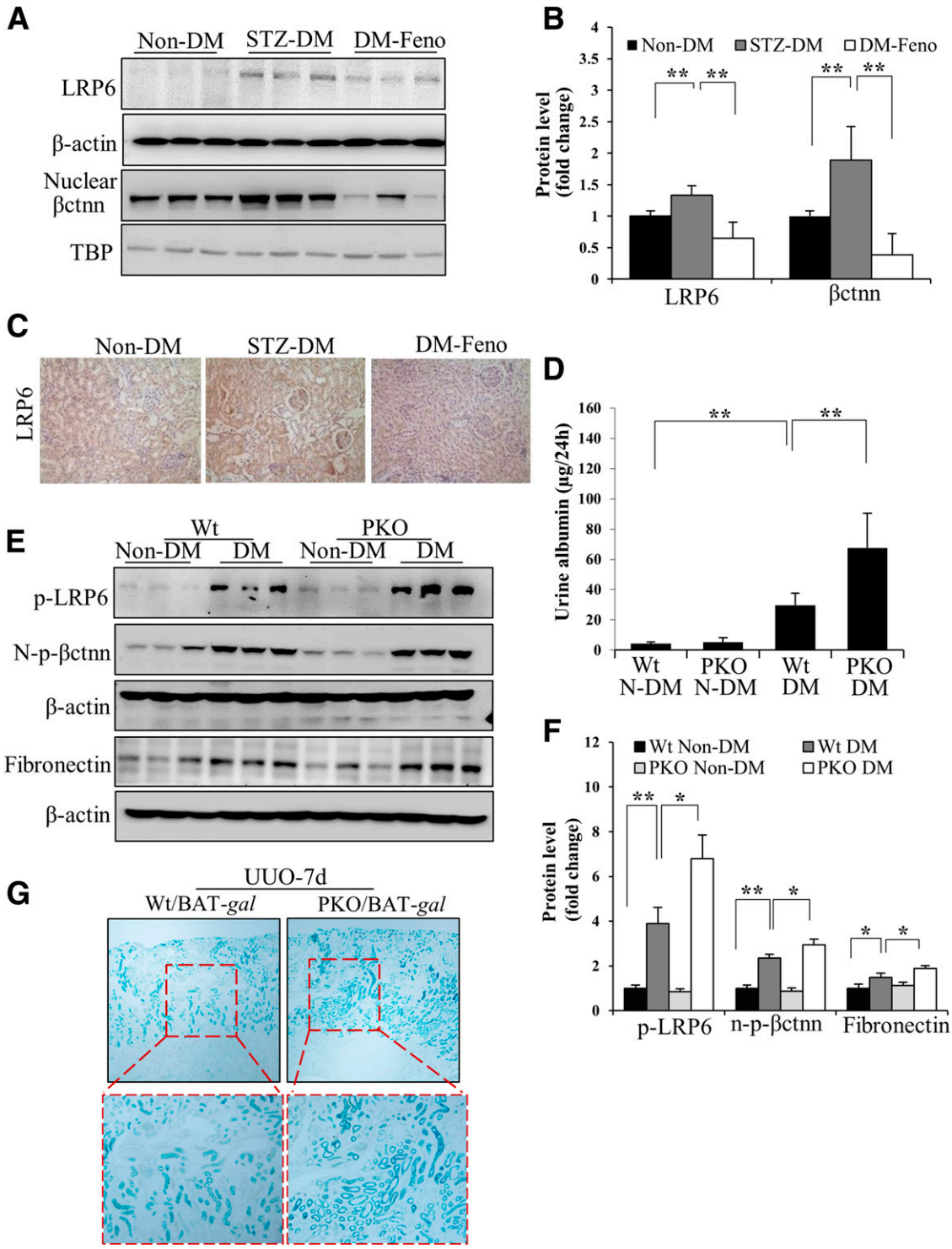

Figure 5—Inhibitory effects of PPARα activation on Wnt signaling in renal fibrosis models. Representative Western blots (*A*) and densitometry analyses (*B*) show levels of total LRP6 and nuclear β-catenin (βctnn) in the renal cortex in nondiabetic rats (Non-DM) and STZ-diabetic rats with fenofibrate chow (DM-Feno) or control chow (STZ-DM). $n = 4$ in Non-DM and STZ-DM; $n = 6$ in DM-Feno. *C*: Representative images of immunohistochemical staining (brown) show changes in renal LRP6 levels in the diabetic rats treated with fenofibrate (original magnification ×200). *D*: ELISA results show albumin levels in 24-h urine samples in diabetic PPARα$^{-/-}$ mice (PKO) and age-matched Wt mice. $n = 6$. Representative Western blots (*E*) and semiquantitative analyses (*F*) compare levels of renal p-LRP6, N-p-β-catenin (N-p-βctnn), and fibronectin in diabetic and nondiabetic PKO mice and age-matched Wt mice. $n = 6$. *G*: PPARα$^{-/-}$/BAT-*gal* mice (PKO/BAT-*gal*) and their Wt/BAT-*gal* littermates (Wt/BAT-*gal*) received UUO. The kidney with UUO was subjected to X-gal staining (blue) at postoperation day 7 to detect the transcriptional activity of β-catenin in the kidney (original magnification: top panels, ×40; bottom panels, higher magnification of the boxed areas). TBP, TATA-binding protein. $n = 3$. Values are reported as the mean ± SD. $^*P < 0.05$ and $^{**}P < 0.01$.

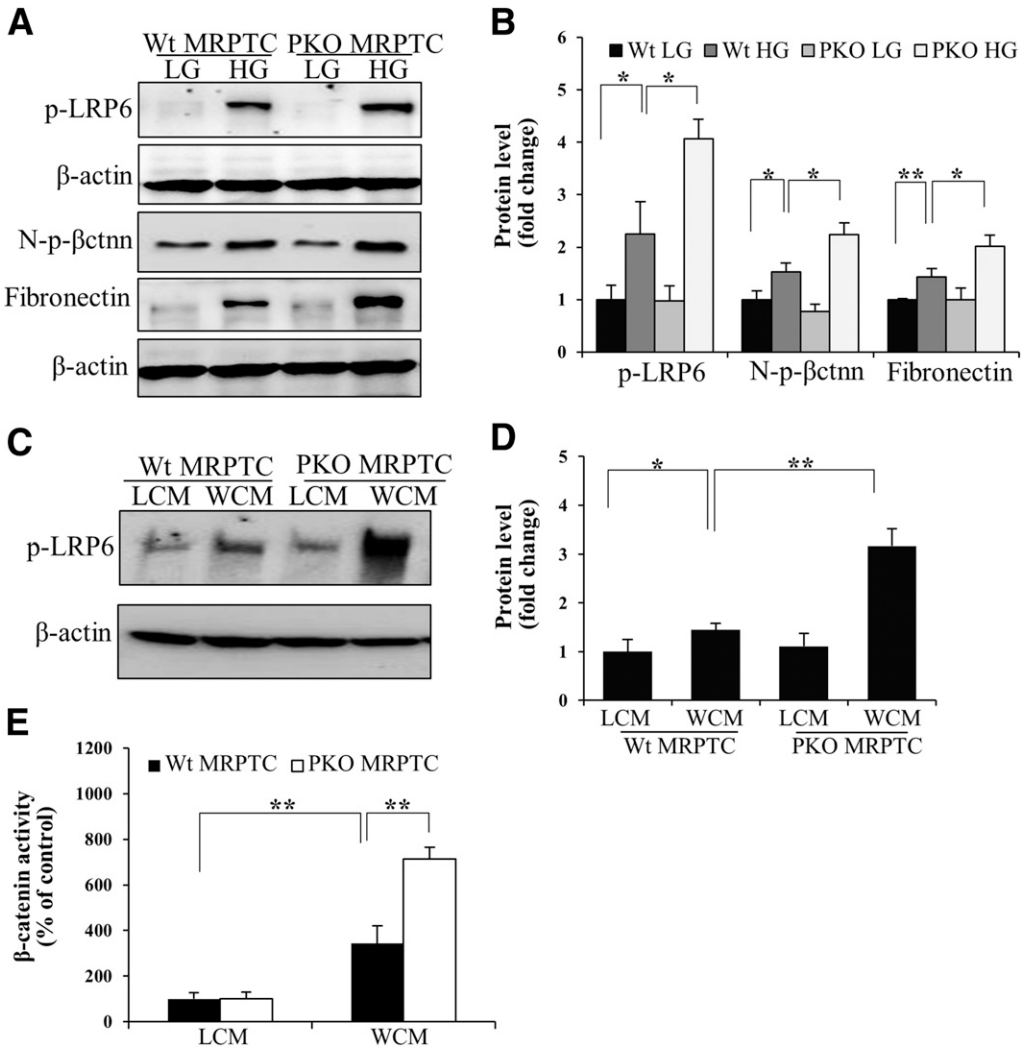

Figure 6—Deficiency of PPARα-promoted Wnt pathway activation in proximal tubular cells. Primary mouse renal proximal tubular cells (MRPTC) were isolated and cultured from 21-day-old PPARα$^{-/-}$ mice (PKO) and Wt littermates. Representative Western blots (*A*) and semiquantitative analyses (*B*) of p-LRP6, N-p-β-catenin (N-p-βctnn), and fibronectin in primary MRPTCs treated with 30 mmol/L D-glucose (high glucose [HG]) for 72 h, with the 5 mmol/L D-glucose plus 25 mmol/L L-glucose (low glucose [LG]) as a control. WCM-induced phosphorylation of LRP6 was measured by Western blot analysis (*C*) and semiquantitative analysis (*D*) in primary MRPTCs. *E*: Luciferase assay was used to measure the transcriptional activity of β-catenin in Wt and PPARα$^{-/-}$ MRPTCs. LCM, L-cell conditioned medium. Values are reported as the mean ± SD. n = 3–4. *P < 0.05 and **P < 0.01.

suggested that PPARα inhibits the canonic Wnt pathway at the Wnt receptor level.

PPARα Decreased LRP6 Stability Through Antioxidant Effects

LRP6 is a crucial coreceptor in the canonic Wnt pathway. To determine whether the regulation of PPARα on Wnt signaling is accomplished through the modulation of LRP6, we measured the protein stability of LRP6 in renal proximal tubular cells. Overexpression of PPARα significantly accelerated degradation of LRP6 protein, as shown in the protein stability assay (Fig. 7*C*). In contrast, primary proximal tubular cells from PPARα$^{-/-}$ mice showed a delayed degradation and prolonged half-life of LRP6, compared with Wt cells (Fig. 7*D*). These data suggested that PPARα inhibits the canonic Wnt pathway through regulating LRP6 protein stability.

We have previously demonstrated that oxidative stress contributes to the activation of the canonic Wnt pathway through stabilizing LRP6 both in retinal pigment epithelial cells (30) and in HKC8 cells (Supplementary Fig. 3). To investigate whether PPARα decreases the stability of LRP6 through reducing oxidative stress, we measured ROS levels in cultured proximal tubular cells. Overexpression of PPARα significantly inhibited ROS generation induced by 4-HNE, a major lipid peroxidation product (Fig. 8*A*). On the other hand, deficiency of PPARα resulted in more prominent increases in 4-HNE–induced intracellular ROS levels (Fig. 8*B*). These results suggested that PPARα inhibits the canonic

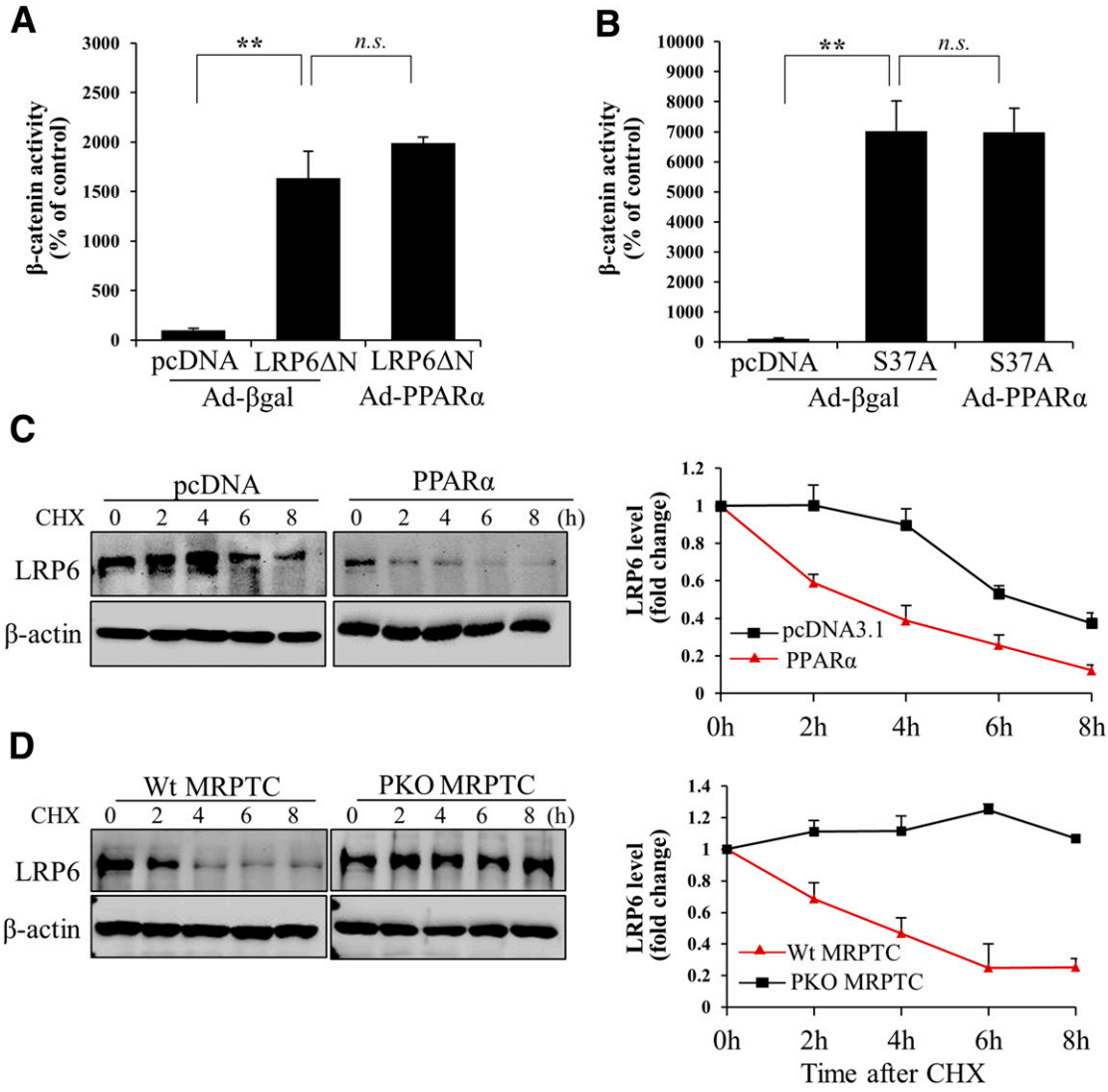

Figure 7—PPARα inhibits the canonic Wnt pathway through destabilizing LRP6. HKC-8 TOPFLASH cells were transfected with plasmids expressing LRP6ΔN (*A*) or a constitutively active mutant of β-catenin (S37A) (*B*), then were infected with Ad-PPARα for another 24 h. Transcriptional activity of β-catenin was measured using a luciferase assay. Twenty-four hours after transfection with a plasmid expressing PPARα, the cells were treated with WCM for 24 h, then incubated with cycloheximide (CHX; 50 μmol/L) for the indicated times. *C*: Levels of LRP6 in cell lysates were measured using Western blot analysis. Primary mouse renal proximal tubular cells (MRPTCs) were cultured from PPARα$^{-/-}$ mice (PKO) and age-matched Wt mice. Cells were incubated with WCM for 24 h and then treated with CHX for the indicated times. *D*: LRP6 stability was measured by Western blot analysis. Values are reported as the mean ± SD, $n = 3$. $^{**}P < 0.01$. n.s., no significance. Ad-βgal, Ad-expressing β-galactosidase.

Wnt pathway through promoting LRP6 protein degradation, which is mediated by its antioxidant activities.

To delineate the underlying mechanism for the antioxidant activities of PPARα, we examined the expression levels of NOX4, a key enzyme responsible for ROS generation in DN. Hyperglycemia increased NOX4 expression levels in HKC-8 cells (Fig. 8*C* and *D*). Diabetic PPARα$^{-/-}$ mice showed more prominent NOX4 overexpression in the kidney, compared with diabetic Wt mice (Fig. 8*E* and *F*). To evaluate the effect of NOX4 on the activation of the Wnt pathway, the transcriptional activity of β-catenin was measured. Overexpression of NOX4 using an adenoviral vector significantly enhanced Wnt3a-induced Wnt signaling pathway (Fig. 8*G*). These data suggested that PPARα regulates the canonic Wnt pathway, at least in part, through inhibiting the NOX4/ROS pathway in renal cells.

DISCUSSION

PPARα agonists have displayed therapeutic effects on DN (8). The aberrant activation of the Wnt signaling pathway has been identified to play a crucial role in renal fibrosis (11–13,31). Tissue- and organ-specific interactions between the Wnt signaling pathway and PPARγ have been reported (32,33). However, the role of PPARα in the

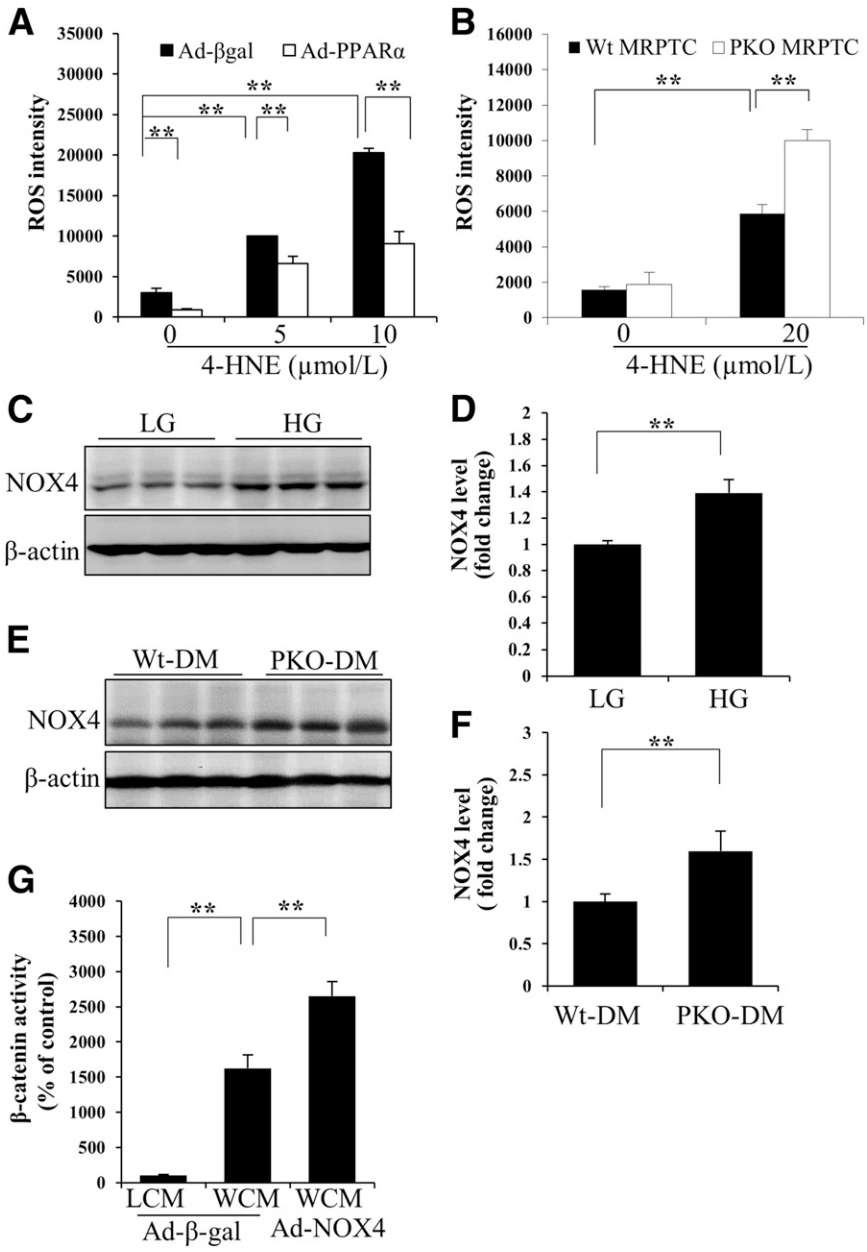

Figure 8—Antioxidant effects of PPARα. Levels of intracellular ROS in HKC-8 cells infected with Ad-PPARα (*A*) or in primary mouse renal proximal tubular cells (MRPTCs) from PPARα$^{-/-}$ (PKO) and Wt (*B*) mice were determined using CM-H_2DCFDA staining (n = 4–5). Ad-β-galactosidase (Ad-βgal) was used as a control virus. Representative Western blots (*C*) and semiquantitative analyses (*D*) show NOX4 levels in HRPTCs treated with 30 mmol/L D-glucose (high glucose [HG]) or 5 mmol/L D-glucose plus 25 mmol/L L-glucose (low glucose [LG]) for 72 h (n = 3). Representative Western blots of NOX4 levels in the renal cortex from STZ-diabetic Wt (Wt-DM) and diabetic PPARα$^{-/-}$ (PKO-DM) mice (*E*) and densitometry analysis (*F*) (n = 5). *G*: Luciferase assay shows the effect of overexpression of NOX4 using Ad-NOX4 infection on transcriptional activity of β-catenin in the presence of WCM. n = 4. LCM, L-cell conditioned medium. Values are reported as the mean ± SD. $^{**}P < 0.01$.

regulation of the Wnt signaling pathway has not been previously documented. The current study demonstrated that fenofibrate, a PPARα agonist, ameliorates proteinuria and renal fibrosis, and inhibits aberrant activation of the canonical Wnt pathway in the kidneys of diabetic rats. Activation and overexpression of PPARα significantly inhibit Wnt signaling induced by diabetic conditions and by a Wnt ligand in cultured renal cells. In contrast, the ablation of PPARα results in a more prominent activation of the canonic Wnt pathway in the kidneys of both DN and obstructive nephropathy models. Because the expression of PPARα was downregulated in the kidneys of both type 1 and type 2 diabetic animal models, the reduced renal PPARα levels may be responsible, at least in part, for the overactivation of Wnt signaling in the kidney of diabetic models, contributing to renal inflammation and fibrosis in DN. Toward the molecular basis by which PPARα regulates Wnt signaling, the current study demonstrated that PPARα destabilizes the crucial Wnt coreceptor LRP6 through

inhibiting the renal NOX4/ROS production. These observations provide the first evidence that PPARα functions as a negative regulator of Wnt signaling in the kidney, and reveal a new mechanism responsible for the anti-inflammatory and antifibrogenic activities of PPARα.

Members in the PPAR family control distinct signaling pathways by regulating specific gene cassettes. In the PPAR family, PPARγ is highly produced in adipose tissue and regulates lipogenesis, and PPARα is mainly expressed in tissues with high mitochondrial and β-oxidation activities (34). It has been reported (35,36) that PPARγ inhibited Wnt signaling in adipogenesis and kidney diseases, partly through downregulating the levels of β-catenin. Recently, the PPARα antagonist MK886 was reported to increase the expression level of β-catenin in cocultured spheroid and endometrial cells (37), and the activation of the Wnt/β-catenin pathway inhibits PPARα-mediated induction of cytochrome p450 genes (38). In the current study, we demonstrate an inhibitory effect of PPARα on Wnt signaling using gain-of-function and loss-of-function approaches. Using a constitutively active LRP6 mutant and β-catenin mutant, we confirmed that the inhibition of the Wnt pathway by PPARα does not occur intracellularly. We found that PPARα decreases the protein stability of LRP6, which could be partly reversed by the ubiquitination inhibitor MG132 (Supplementary Fig. 4*A*), suggesting that PPARα-induced LRP6 degradation occurs partly through promoting ubiquitination of LRP6 in kidney. LRP6 plays a crucial role in Wnt signaling overactivation in diabetes, because the blockade of LRP6 alone is sufficient to attenuate Wnt signaling overactivation and to ameliorate diabetic retinopathy and DN (12,17). Thus, the destabilization of LRP6 is likely responsible for the inhibitory effect of PPARα on Wnt signaling, suggesting that PPARα interacts with the Wnt pathway at a different target than that of PPARγ.

Fenofibrate has been reported to have therapeutic effects on DN both in human patients with diabetes and in diabetic animal models (8,39). However, a unifying mechanism that is responsible for the anti-inflammatory and antifibrotic effects of fenofibrate remains unclear. The Wnt pathway has been shown to mediate inflammation through upregulation of inflammatory factors, such as tumor necrosis factor-α and intracellular adhesion molecule-1, and to enhance fibrosis through upregulation of CTGF and fibronectin (40,41). Previous studies (11,12,31,42) have shown that the overactivation of Wnt signaling, as found in both type 1 and type 2 diabetic models, plays a crucial role in renal dysfunction in DN. We found that fenofibrate promoted PPARα-induced degradation of LRP6, without changing the mRNA levels (Supplementary Fig. 4*C–E*). Therefore, suppression of Wnt signaling overactivation by PPARα may represent a mechanism for the anti-inflammatory and antifibrotic effects of fenofibrate.

Hyperglycemia-induced oxidative stress is considered the primary cause of tissue damage in DN (43). The antioxidant effects of PPARα and its agonist have been reported in the retinae and kidneys of diabetic models by our group and others (8,19,44). We have reported (30) that enhanced oxidative stress contributed to the activation of the Wnt pathway in the retinae of diabetic rats via stabilizing LRP6. In our study, 4-HNE–induced ROS production was significantly inhibited by the overexpression of PPARα. PPARα deficiency dramatically enhanced 4-HNE–induced ROS generation. These observations suggest that the antioxidant effects of PPARα in the kidney result in the destabilization of LRP6, which leads to the inhibition of Wnt signaling.

The NOX family is believed to be one of the major oxidases regulating ROS production in DN (45,46). NOX4 is a crucial isoform contributing to DN, because the deficiency of NOX1 and NOX2 has no effect on the albuminuria and renal fibrosis in diabetic animals (47,48). In contrast, mice with NOX4 knockout or that have been treated with NOX4 inhibitors showed ameliorated urine albumin excretion and downregulation of renal fibrosis–related proteins in a long duration of diabetes (48–50). In the current study, diabetic PPARα$^{-/-}$ mice showed significantly higher levels of NOX4 compared with diabetic Wt mice, demonstrating that PPARα negatively regulates NOX4 expression. We have previously identified that fenofibrate suppressed the expression of NOX4 in retinal pericytes (19). In this study, we have demonstrated that the overexpression of NOX4 significantly enhanced Wnt3a-induced transcriptional activity of β-catenin, suggesting that the negative regulation of NOX4 by PPARα may contribute to the inhibition of Wnt signaling. However, the detailed molecular mechanism responsible for the regulation of NOX4 by PPARα remains to be studied further.

Our results showed that nondiabetic PPARα$^{-/-}$ mice lack significant changes in renal levels of p-LRP6 and N-p-β-catenin, suggesting that PPARα deficiency is not sufficient to activate Wnt signaling under nondiabetic conditions. This notion is supported by observations of primary renal cells, which showed that PPARα deficiency alone does not activate the Wnt pathway under normal glucose medium or in the absence of Wnt ligands. ROS generation in the PPARα$^{-/-}$ cells was increased only in the presence of 4-HNE and not in vehicle control. These results suggest that PPARα only inhibits the activation of Wnt signaling under stress conditions, such as oxidative stress, and the mechanism remains unclear.

In summary, we identified that PPARα confers a renal protective effect through blocking activation of the canonic Wnt pathway in DN. This inhibitory effect of PPARα on Wnt signaling occurs through destabilizing LRP6, which is mediated by the antioxidant activity of PPARα. This finding suggests that the interaction between PPARα and the canonic Wnt pathway renders a new therapeutic target for renal fibrosis.

Funding. This study was supported by National Institutes of Health grants EY-012231, EY-018659, EY-019309, and GM-104934; Oklahoma Center for the Advancement of Science and Technology grants HR12-103 and HR13-076A; and JDRF grants 3-PDF-2014-107-A-N and 2-SRA-2014-147-Q-R.

Duality of Interest. No potential conflicts of interest relevant to this article were reported.

Author Contributions. R.C. contributed to designing and performing most of the experiments, data analysis, and manuscript writing. L.D. assisted in animal studies. X.H. purified adenoviruses and assisted in animal studies. Y.T. made and provided the adenoviruses and plasmids used in this study. J.-x.M. designed and directed the study and contributed to writing and editing the manuscript. J.-x.M. is the guarantor of this work and, as such, had full access to all the data in the study and takes responsibility for the integrity of the data and the accuracy of the data analysis.

References

1. Molitch ME, DeFronzo RA, Franz MJ, et al.; American Diabetes Association. Nephropathy in diabetes. Diabetes Care 2004;27(Suppl. 1):S79–S83
2. Raptis AE, Viberti G. Pathogenesis of diabetic nephropathy. Exp Clin Endocrinol Diabetes 2001;109(Suppl. 2):S424–S437
3. Estacio RO, Schrier RW. Diabetic nephropathy: pathogenesis, diagnosis, and prevention of progression. Adv Intern Med 2001;46:359–408
4. Desvergne B, Wahli W. Peroxisome proliferator-activated receptors: nuclear control of metabolism. Endocr Rev 1999;20:649–688
5. Forsblom C, Hiukka A, Leinonen ES, Sundvall J, Groop PH, Taskinen MR. Effects of long-term fenofibrate treatment on markers of renal function in type 2 diabetes: the FIELD Helsinki substudy. Diabetes Care 2010;33:215–220
6. Ismail-Beigi F, Craven T, Banerji MA, et al.; ACCORD trial group. Effect of intensive treatment of hyperglycaemia on microvascular outcomes in type 2 diabetes: an analysis of the ACCORD randomised trial. Lancet 2010;376:419–430
7. Wright AD, Dodson PM. Medical management of diabetic retinopathy: fenofibrate and ACCORD Eye studies. Eye (Lond) 2011;25:843–849
8. Balakumar P, Kadian S, Mahadevan N. Are PPAR alpha agonists a rational therapeutic strategy for preventing abnormalities of the diabetic kidney? Pharmacol Res 2012;65:430–436
9. Park CW, Kim HW, Ko SH, et al. Accelerated diabetic nephropathy in mice lacking the peroxisome proliferator-activated receptor alpha. Diabetes 2006;55:885–893
10. Logan CY, Nusse R. The Wnt signaling pathway in development and disease. Annu Rev Cell Dev Biol 2004;20:781–810
11. Rooney B, O'Donovan H, Gaffney A, et al. CTGF/CCN2 activates canonical Wnt signalling in mesangial cells through LRP6: implications for the pathogenesis of diabetic nephropathy. FEBS Lett 2011;585:531–538
12. Zhou T, He X, Cheng R, et al. Implication of dysregulation of the canonical wingless-type MMTV integration site (WNT) pathway in diabetic nephropathy. Diabetologia 2012;55:255–266
13. Kato H, Gruenwald A, Suh JH, et al. Wnt/β-catenin pathway in podocytes integrates cell adhesion, differentiation, and survival. J Biol Chem 2011;286:26003–26015
14. Zhang SX, Ma JX, Sima J, et al. Genetic difference in susceptibility to the blood-retina barrier breakdown in diabetes and oxygen-induced retinopathy. Am J Pathol 2005;166:313–321
15. Tan R, Zhang X, Yang J, Li Y, Liu Y. Molecular basis for the cell type specific induction of SnoN expression by hepatocyte growth factor. J Am Soc Nephrol 2007;18:2340–2349
16. Li H, Zhou X, Davis DR, Xu D, Sigmund CD. An androgen-inducible proximal tubule-specific Cre recombinase transgenic model. Am J Physiol Renal Physiol 2008;294:F1481–F1486
17. Lee K, Hu Y, Ding L, et al. Therapeutic potential of a monoclonal antibody blocking the Wnt pathway in diabetic retinopathy. Diabetes 2012;61:2948–2957
18. Racusen LC, Monteil C, Sgrignoli A, et al. Cell lines with extended in vitro growth potential from human renal proximal tubule: characterization, response to inducers, and comparison with established cell lines. J Lab Clin Med 1997;129:318–329
19. Ding L, Cheng R, Hu Y, et al. Peroxisome proliferator-activated receptor α protects capillary pericytes in the retina. Am J Pathol 2014;184:2709–2720
20. Zhang J, Yang J, Liu Y. Role of Bcl-xL induction in HGF-mediated renal epithelial cell survival after oxidant stress. Int J Clin Exp Pathol 2008;1:242–253
21. Terryn S, Jouret F, Vandenabeele F, et al. A primary culture of mouse proximal tubular cells, established on collagen-coated membranes. Am J Physiol Renal Physiol 2007;293:F476–F485
22. Liu Q, Li J, Cheng R, et al. Nitrosative stress plays an important role in Wnt pathway activation in diabetic retinopathy. Antioxid Redox Signal 2013;18:1141–1153
23. Park K, Lee K, Zhang B, et al. Identification of a novel inhibitor of the canonical Wnt pathway. Mol Cell Biol 2011;31:3038–3051
24. Vallon V, Thomson SC. Renal function in diabetic disease models: the tubular system in the pathophysiology of the diabetic kidney. Annu Rev Physiol 2012;74:351–375
25. Maretto S, Cordenonsi M, Dupont S, et al. Mapping Wnt/beta-catenin signaling during mouse development and in colorectal tumors. Proc Natl Acad Sci USA 2003;100:3299–3304
26. Surendran K, Schiavi S, Hruska KA. Wnt-dependent beta-catenin signaling is activated after unilateral ureteral obstruction, and recombinant secreted frizzled-related protein 4 alters the progression of renal fibrosis. J Am Soc Nephrol 2005;16:2373–2384
27. He W, Dai C, Li Y, Zeng G, Monga SP, Liu Y. Wnt/beta-catenin signaling promotes renal interstitial fibrosis. J Am Soc Nephrol 2009;20:765–776
28. Liu G, Bafico A, Harris VK, Aaronson SA. A novel mechanism for Wnt activation of canonical signaling through the LRP6 receptor. Mol Cell Biol 2003;23:5825–5835
29. Li Y, Lu W, He X, Bu G. Modulation of LRP6-mediated Wnt signaling by molecular chaperone Mesd. FEBS Lett 2006;580:5423–5428
30. Zhou T, Zhou KK, Lee K, et al. The role of lipid peroxidation products and oxidative stress in activation of the canonical wingless-type MMTV integration site (WNT) pathway in a rat model of diabetic retinopathy. Diabetologia 2011;54:459–468
31. Dai C, Stolz DB, Kiss LP, Monga SP, Holzman LB, Liu Y. Wnt/beta-catenin signaling promotes podocyte dysfunction and albuminuria. J Am Soc Nephrol 2009;20:1997–2008
32. Lecarpentier Y, Claes V, Duthoit G, Hébert JL. Circadian rhythms, Wnt/beta-catenin pathway and PPAR alpha/gamma profiles in diseases with primary or secondary cardiac dysfunction. Front Physiol 2014;5:429
33. Nagao S, Yamaguchi T. PPAR-γ agonists in polycystic kidney disease with frequent development of cardiovascular disorders. Curr Mol Pharmacol 2012;5:292–300
34. Guan Y, Breyer MD. Peroxisome proliferator-activated receptors (PPARs): novel therapeutic targets in renal disease. Kidney Int 2001;60:14–30
35. Lee YJ, Han HJ. Troglitazone ameliorates high glucose-induced EMT and dysfunction of SGLTs through PI3K/Akt, GSK-3β, Snail1, and β-catenin in renal proximal tubule cells. Am J Physiol Renal Physiol 2010;298:F1263–F1275
36. Moldes M, Zuo Y, Morrison RF, et al. Peroxisome-proliferator-activated receptor gamma suppresses Wnt/beta-catenin signalling during adipogenesis. Biochem J 2003;376:607–613
37. Tsang H, Cheung TY, Kodithuwakku SP, et al. Perfluorooctanoate suppresses spheroid attachment on endometrial epithelial cells through peroxisome proliferator-activated receptor alpha and down-regulation of Wnt signaling. Reprod Toxicol 2013;42:164–171
38. Thomas M, Bayha C, Vetter S, et al. Activating and Inhibitory Functions of WNT/β-Catenin in the Induction of Cytochromes P450 by Nuclear Receptors in HepaRG Cells. Mol Pharmacol 2015;87:1013–1020
39. Ansquer JC, Foucher C, Aubonnet P, Le Malicot K. Fibrates and microvascular complications in diabetes—insight from the FIELD study. Curr Pharm Des 2009;15:537–552
40. Zhou T, Hu Y, Chen Y, et al. The pathogenic role of the canonical Wnt pathway in age-related macular degeneration. Invest Ophthalmol Vis Sci 2010;51:4371–4379
41. Zhang B, Zhou KK, Ma JX. Inhibition of connective tissue growth factor overexpression in diabetic retinopathy by SERPINA3K via blocking the WNT/β-catenin pathway. Diabetes 2010;59:1809–1816

42. Duan S, Wu Y, Zhao C, et al. The wnt/β-catenin signaling pathway participates in rhein ameliorating kidney injury in DN mice. Mol Cell Biochem 2016;411:73–82
43. Brownlee M. The pathobiology of diabetic complications: a unifying mechanism. Diabetes 2005;54:1615–1625
44. Moran E, Ding L, Wang Z, et al. Protective and antioxidant effects of PPARα in the ischemic retina. Invest Ophthalmol Vis Sci 2014;55:4568–4576
45. Kashihara N, Haruna Y, Kondeti VK, Kanwar YS. Oxidative stress in diabetic nephropathy. Curr Med Chem 2010;17:4256–4269
46. Holterman CE, Read NC, Kennedy CR. Nox and renal disease. Clin Sci (Lond) 2015;128:465–481
47. You YH, Okada S, Ly S, et al. Role of Nox2 in diabetic kidney disease. Am J Physiol Renal Physiol 2013;304:F840–F848
48. Jha JC, Gray SP, Barit D, et al. Genetic targeting or pharmacologic inhibition of NADPH oxidase nox4 provides renoprotection in long-term diabetic nephropathy. J Am Soc Nephrol 2014;25:1237–1254
49. Thallas-Bonke V, Jha JC, Gray SP, et al. Nox-4 deletion reduces oxidative stress and injury by PKC-α-associated mechanisms in diabetic nephropathy. Physiol Rep 2014;2(11):e12192
50. Babelova A, Avaniadi D, Jung O, et al. Role of Nox4 in murine models of kidney disease. Free Radic Biol Med 2012;53:842–853